Communication: Strong excitonic and vibronic effects determine the optical properties of LiO

García Lastra, Juan Maria; Bass, J. D.; Thygesen, Kristian Sommer

Published in:
Journal of Chemical Physics

Link to article, DOI:
10.1063/1.3645544

Publication date:
2011

Document Version
Publisher's PDF, also known as Version of record

Communication: Strong excitonic and vibronic effects determine the optical properties of Li2O2

J. M. Garcia-Lastra, J. D. Bass, and K. S. Thygesen

Citation: J. Chem. Phys. **135**, 121101 (2011); doi: 10.1063/1.3645544
View online: http://dx.doi.org/10.1063/1.3645544
View Table of Contents: http://jcp.aip.org/resource/1/JCPSA6/v135/i12
Published by the American Institute of Physics.

Communication: Strong excitonic and vibronic effects determine the optical properties of Li_2O_2

J. M. Garcia-Lastra,[1,a)] J. D. Bass,[2] and K. S. Thygesen[1]
[1]*Center for Atomic-scale Materials Design (CAMD), Department of Physics, Technical University of Denmark, Fysikvej 1, 2800 Kgs. Lyngby, Denmark*
[2]*IBM Research – Almaden, 650 Harry Road, San José, California 95120, USA*

(Received 11 August 2011; accepted 13 September 2011; published online 28 September 2011)

The band structure and optical absorption spectrum of lithium peroxide (Li_2O_2) is calculated from first-principles using the G_0W_0 approximation and the Bethe-Salpeter equation, respectively. A strongly localized (Frenkel type) exciton corresponding to the $\pi^* \rightarrow \sigma^*$ transition on the O_2^{-2} peroxide ion gives rise to a narrow absorption peak around 1.2 eV below the calculated bandgap of 4.8 eV. In the excited state, the internal O_2^{-2} bond is significantly weakened due to the population of the σ^* orbital. As a consequence, the bond is elongated by almost 0.5 Å leading to an extreme Stokes shift of 2.6 eV. The strong vibronic coupling entails significant broadening of the excitonic absorption peak in good agreement with diffuse reflectance data on Li_2O_2 which shows a rather featureless spectrum with an absorption onset around 3.0 eV. These results should be important for understanding the origin of the high potential losses and low current densities, which are presently limiting the performance of Li-air batteries. © *2011 American Institute of Physics*. [doi:10.1063/1.3645544]

The development of non-aqueous Li-air batteries in the late 1990s and the rapidly growing demands for better and more sustainable methods for energy storage, have recently spurred a great deal of interest in the material Li_2O_2.[1–4] The formation of Li_2O_2 at the cathode of these Li-air batteries during discharge was confirmed by Raman spectroscopy which showed a characteristic peak at 795 cm^{-1}, corresponding to the stretching mode of the O_2^{2-} peroxide ion.[1] This peak is a common feature in all the alkali and alkali-earth peroxides and indicates a decoupling of the peroxide ions from the rest of the lattice.[5] The main limiting factor in the performance of reversible Li-air batteries, namely, the large potential losses at realistic current densities, is believed to be related to poor intrinsic transport properties of Li_2O_2 and/or the metal or carbon-Li_2O_2 interface.[6] Here we apply optical spectroscopy to demonstrate a very strong localization of the electron-hole (e-h) pairs in Li_2O_2. The strong localization of the e–h pairs furthermore leads to huge vibronic effects. This suggests that the electronic structure of Li_2O_2 is similar to that of molecular solids, which are generally poorly conducting with the charge transport mechanism being hopping rather than band-like.

The optical spectrum of the O_2^{2-} ion in the bulk of ionic lattices was investigated in Na_2O_2 commercial samples by Griffiths *et al.*[7] in 1959. However, the presence of 10% of superoxide ions (O_2^-) in the samples made it difficult to identify the origin of different features in the spectrum. Andersen *et al.* studied the optical spectrum of the O_2^{2-} ion in doped KCl:O_2.[8] They observed a broadband of width ~0.5 eV peaking at 4.77 eV in the absorption spectrum and a broadband of width ~0.3 eV peaking at 3.14 eV in the emission spectrum. This noticeable Stokes shift (1.63 eV) and the broadening of the bands are fingerprints of a strong vibronic coupling related to the O_2^{2-} ion in the light absorption process. However, to the authors' knowledge no theoretical study has so far confirmed or quantified this picture.

In this letter, we present a combined experimental and theoretical study of the optical properties of Li_2O_2. Our results demonstrate that the broad and featureless absorption spectrum observed experimentally and the low (compared to the 4.8 eV bandgap) absorption onset around 3 eV can be explained by the combined effects of strong electron-hole and electron-phonon couplings. The strong excitonic and vibronic couplings arise from the decoupled nature of the O_2^{2-} ions from the rest of the lattice. The valence and conduction bands are comprised almost entirely of the π^* and σ^* orbitals of the O_2^{2-} ions, respectively, with almost no contribution from the Li states. This leads to highly localized excitonic states which in turn cause large local distortions of the lattice.

Solid-state UV/Vis spectroscopy was performed on Li_2O_2 at room temperature (RT) on a Cary 5000 spectrophotometer equipped with a Labsphere DRA-2500 in diffuse reflectance mode. Data were acquired in the region of 800–190 nm using Teflon as a reference. Finely, powdered Li_2O_2 (Aldrich, 99.9% pure) was transferred in a glovebox (<0.1 parts per million H_2O and O_2) to an o-ring sealed cell of 1mm thickness that contained suprasil quartz windows. Data were collected in double-beam mode using a reduced slit height, a scan rate of 600 nm/min, 0.1 s averaging and with a spectromer bandwidth of 2.0 nm. The data were zeroed based on the measurement at 800 nm. The diffuse reflectance data were converted to absorbance using the Kubelka-Munk formalism, which provides a linear correlation with the molar absorptivity.[9] No corrections were included for the small absorption and specular reflection due to the quartz window. Luminescence experiments were carried out, also at RT. However, we found that the luminescence of Li_2O_2 is quenched at RT.

a)Author to whom correspondence should be addressed. Electronic mail: jumagala@fysik.dtu.dk.

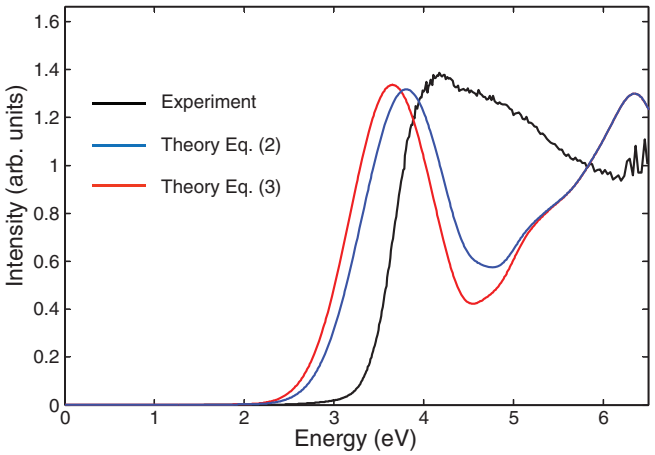

FIG. 1. Experimental (black) and theoretical spectra of Li_2O_2. Two theoretical spectra are shown, one derived from the full Born-Oppenheimer approximation (blue, see Eq. (2)) and the other from the Franck-Condon approximation (red, see Eq. (3)).

Theoretical calculations of the absorption spectrum were performed by solving the Bethe-Salpeter equation (BSE)[10,11] with G_0W_0 – corrected single-particle energies[11–13] following the procedure described in Ref. 14. Density functional theory calculations were carried out by means of the QUANTUM-ESPRESSO code,[15] using the Li_2O_2 structure proposed by Cota and de la Mora[16] (see Fig. 2). The exchange-correlation energy was computed with the Perdew-Burke-Ernzehoff (PBE) functional.[17] The ion cores were represented by norm-conserving pseudopotential and a 70 Ry plane wave cutoff was used for the wave functions. The Brillouin zone was sampled on a $6 \times 6 \times 4$ Monkhorst–Pack grid.[18] The G_0W_0 corrections were computed with the YAMBO code,[19] using a 70 eV cutoff for the sum over virtual states. The plasmon pole approximation[13] was employed and local field effects were included using 1000 G vectors (equivalent to an energy cutoff of 7 Ry). We have checked that the QP gap is converged to within 0.1 eV with respect to the energy cutoff used for virtual states and local field effects.

The analysis of the partial density of states (PDOS) in Fig. 3 constructed from the G_0W_0-corrected PBE calculations

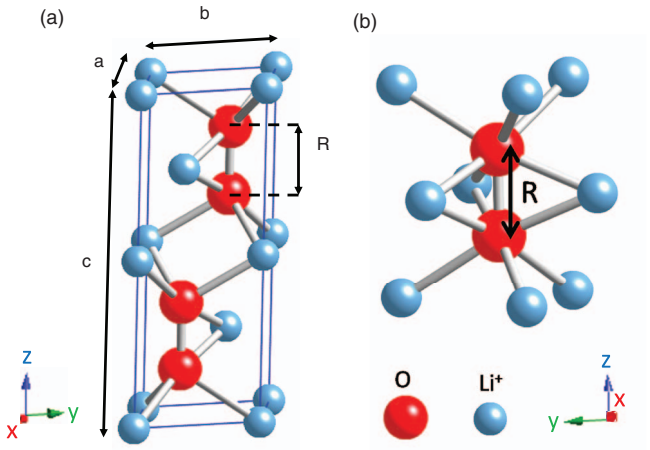

FIG. 2. (a) Li_2O_2 unit cell taken from Ref. 16. Lattice parameters a = b = 3.187 Å, c = 7.7258 Å. (b) $O_2Li_9^{7+}$ cluster (11 ions) used in ADF calculations.

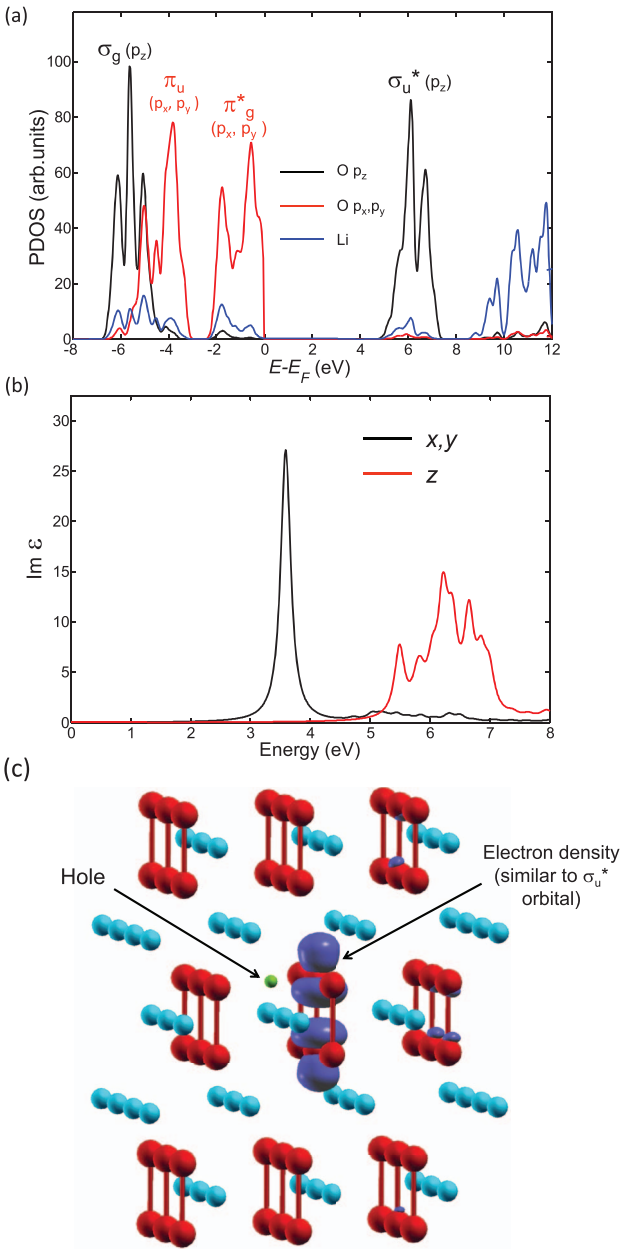

FIG. 3. (a) G_0W_0 calculated partial densities of states (PDOS) of Li_2O_2 for oxygen p_z (black), p_x (red) and lithium (blue) contributions. Due to the symmetry of the system, the oxygen p_x and p_y PDOS are identical. The different peaks are identified as the σ_g, σ^*_u, π^*_g, and π_u molecular orbitals of the O_2^{2-} ion. (b) Imaginary part of the dielectric constant obtained from the BSE for light polarizations in the **x**, **y** (black) and **z** (red) directions. Notice that all the peaks are smeared by 0.1 eV. (c) Electronic exciton (dark blue regions) produced in Li_2O_2 when an electronic hole (green sphere) is created at the point in which the electronic density of the π^*_g orbital of one of the O_2^{2-} ions is maximum. Notice that the electronic exciton corresponds almost entirely to the σ^*_u orbital of the same O_2^{2-} ion, with small contributions from the surrounding O_2^{2-} ions.

reveals that the valence and conduction bands of Li_2O_2 almost exclusively involve states on the peroxide ion. The σ_g (O_2^{2-} p_z bonding orbital), the π_u (O_2^{2-} p_x and p_y bonding orbitals), and the π^*_g (O_2^{2-} p_x and p_y antibonding orbitals) orbitals form narrow bands centered at −5.6, −4.1, and −0.8 eV relative to the top of the valence band, respectively. The σ^*_u (O_2^{2-} p_z antibonding orbital) conduction band is centered

at 6.3 eV. The calculated G_0W_0 direct gap at the Γ point is 4.81 eV, which is similar to previously reported G_0W_0–corrected PBE calculations (4.91 eV) (Ref. 20) and to the one obtained by Zhuravlev *et al.* with B3LYP hybrid functional (4.44 eV).[21] On the other hand, the PBE band structure (not shown), shows a direct gap of 1.94 eV, in good agreement with the local-density approximation result of 1.98 eV reported in Ref. 22 and the PBE value of 1.88 eV reported in Ref. 20.

Figure 3(b) shows the imaginary part of the macroscopic dielectric function obtained from the BSE calculations performed on top of the G_0W_0-corrected PBE transition energies. The spectrum is highly anisotropic showing a broadband centered around 6.2 eV for light polarized along the z direction, and a sharp peak at 3.6 eV for polarizations along the x and y directions (the x and y directions are equivalent in Li_2O_2). This is in sharp contrast to the experimental spectrum which consists of a broadband with no sharp features (Fig. 1). It is thus crucial to analyze the origin of this sharp peak in order to elucidate the discrepancies between the theoretical and experimental spectra. The fact that the peak appears only for x and y polarizations indicates that it involves transitions from the π^*_g band to the σ^*_u band, which are dipole forbidden for z polarized light. Furthermore, the large difference between the direct photoemission gap (4.81 eV) and the optical gap (3.6 eV) shows a strong electron-hole interaction, which is the fingerprint of a strongly localized excitation. To more explicitly confirm this scenario we diagonalized the BSE two-particle Hamiltonian to obtain the electron-hole wavefunction corresponding to the energy of the sharp peak. In Fig. 3(c) we plot the absolute value of the excitonic wave function as a function of the electron coordinate. The hole is fixed at a position corresponding to a maximum of the electronic density from the π^*_g band (the hole density), see Refs. 14 and 19 for details of this procedure. It can be seen that the electron density of the excitonic wavefunction corresponds to a σ^*_u orbital localized at the peroxide ion closest to the created hole. Moreover, the exciton is highly localized on a single ion as evidenced by the negligible weight of the excitonic wave function on the surrounding parts of the lattice.

In order to include possible effects on absorption spectrum coming from the coupling to the lattice, we performed delta self-consistent field (ΔSCF) calculations for the excited potential energy surface employing a cluster model of the of Li_2O_2 lattice. We emphasize that both the cluster model and the use of ΔSCF to describe the state is justified by the highly localized nature of the exciton confirmed by the BSE calculations. The ΔSCF calculations were performed with Amsterdam density functional (ADF) code version 2010.[23] One O_2^{2-} peroxide ion and its nine nearest Li^+ neighbors were included in the cluster model (the $O_2Li_9^{7+}$ cluster shown in Fig. 2(b)). The remaining part of the lattice was represented with a set of 292 point charges with values previously fitted to reproduce the electric field corresponding to the infinite system. For more details on this approach we refer to Ref. 24. The PBE functional was used for exchange-correlation energy. All the atoms were described using a TZP basis set (triple-ζ Slater-type orbitals plus one polarization function) and the core electrons were kept frozen. As a test of this

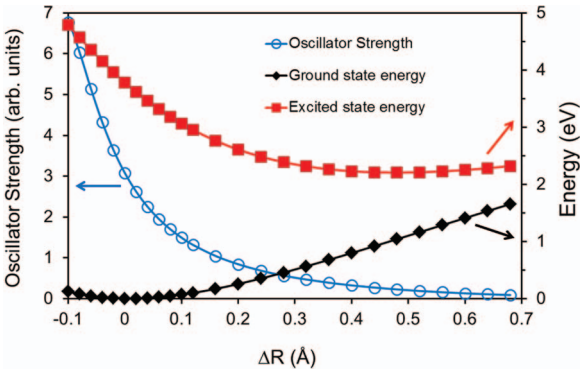

FIG. 4. Calculated energies with the cluster model of the ground (black, right axis) and excited (red, right axis) states of Li_2O_2 as a function of the change of the O–O distance with respect to the relaxed ground state value ($R_0 = 1.55$ Å), ΔR. The oscillator strength of the transition from the ground state to the excited one is also shown (blue, left axis). The excited state corresponds to the promotion of one electron from the π^*_g orbital of the O_2^{2-} ion to the σ^*_u orbital.

model, we performed a ground state relaxation of the O–O bond distance, R, keeping the Li^+ ions frozen at their lattice positions. We obtained a minimum value of $R_0 = 1.55$ Å, the same distance proposed by Cota and de la Mora.[16] We proceed by calculating the excitation energy and the oscillator strength (in x and y directions) of the electronic transition from the ground state of the O_2^{2-} ion to the excited state as a function of R. The excited state was obtained by promoting one electron from the π^*_g orbital of the O_2^{2-} ion to the σ^*_u orbital during the ΔSCF procedure. It should be noticed that this cluster model only keeps its validity if the electronic density remains in the O_2^{2-} ion. If the electronic density is spread to the Li^+ ions it would mean that the electrons start to be delocalized on the lattice, which obviously is not properly described within a cluster model. For the ground state this delocalization problem does not occur in the range of the studied R (from 1.35 Å to 2.25 Å). This is not the case for the excited state, where the delocalization begins to appear for $R < 1.45$ Å. This is due to the destabilization of the O_2^{2-} σ^*_u orbital that takes place when the O–O distance is shortened. This shortening eventually produces an energetic cross between the O_2^{2-} σ^*_u orbital and the Li levels.

Within this model the excitation energy at the equilibrium distance of the ground state, R_0 is 3.78 eV (Fig. 4(a)), which is reasonably close to the value of 3.6 eV obtained from the BSE. Remarkably, the equilibrium O–O distance in the excited state is $R_{exc} = 2.03$ Å, i.e., the displacement with respect to R_0 is $\Delta R = 0.48$ Å (Fig. 4(a)). The excitation energy at R_{exc} is reduced to 1.16 eV, which implies a Stokes shift of 2.62 eV; significantly larger than that observed experimentally for $KCl:O_2^{2-}$ (1.63 eV). The redshift of the Li_2O_2 absorption and emission energies with respect to those of $KCl:O_2^{2-}$ is probably related to the fact that R_0 and R_{exc} are shorter for the latter system. Also the differences in the Madelung potentials of both lattices could contribute to this redshift. From the potential energy curves we obtain the nuclear vibronic wavefunctions (not shown) and the vibrational frequencies for the ground and excited states. For the latter we find 784 cm^{-1} and

500 cm^{-1}, respectively. The ground state frequency is in very good agreement with the experimental figure of 795 cm^{-1}. The variation of the oscillator strength of the $\pi^*_g \rightarrow \sigma^*_u$ transition with respect to R is shown in Fig. 4(b). The observed decay as ΔR increases is due to the fact that the molecular orbitals of the O_2^{2-} ion become more atomic-like when the two O atoms are separated thus converging towards dipole forbidden transitions between atomic p_x/p_y and p_z orbitals. From the vibronic wavefunctions and frequencies and the oscillator strength, the absorption spectrum can be calculated in the Born-Oppenheimer approximation (BOA). In the BOA, the probability, P, of a transition between the ith vibronic ground state and the jth vibronic excited state is given by the expression,

$$P\left(E^j_{\text{exc}} - E^i_{gr}\right) = \left| \int \psi^{j*}_{\text{exc}}(R) \cdot \sqrt{f(R)} \cdot \psi^i_{gr}(R)\, dR \right|^2, \quad (1)$$

where $f(R)$ is the oscillator strength of the electronic transition at the distance R. Since the vibrational energy of the ground state ($\sim$0.1 eV) is four times larger than thermal energy at room temperature, we can take $i = 0$ corresponding to the zero point motion. Thus the probability of a transition at a given energy, $\Delta E = E^j_{exc} - E^0_{gr}$, becomes

$$P(\Delta E) = \left| \int \psi^{j*}_{\text{exc}}(R) \cdot \sqrt{f(R)} \cdot \psi^0_{gr}(R) dR \right|^2. \quad (2)$$

For completeness we note that within the commonly used Franck-Condon approximation (FCA), in which $f(R)$ is assumed to be a constant, f_0, Eq. (2) reduces to[25]

$$P(\Delta E) = f_0 \left| \int \psi^{j*}_{\text{exc}}(R) \cdot \psi^0_{gr}(R) dR \right|^2. \quad (3)$$

We have used Eqs. (2) and (3) to estimate the effect of the vibronic coupling on the excitonic absorption peak obtained for x- and y-polarized light. In order to get the full spectrum we have combined these new results with the ones obtained from the BSE calculation for the z-polarized band. The comparison between the vibronic corrected spectra and the experimental one is shown in Fig. 1. It can be seen that the full BOA and FCA are rather similar. However, the full BOA spectrum is shifted by $\sim$0.2 eV towards higher energies due to the decay in the oscillator strength at low energies. The calculated spectra are in reasonably good agreement with the experimental results. An exception occurs in the region between 4 and 5 eV where the intensity of the theoretical spectrum is smaller than the experimental one. This discrepancy is due to the limitations of model, which becomes invalid for $\Delta R < -0.1$ Å. In this range the transition energies are expected to be in the 4–5 eV range (see Fig. 4) and would thus lead to an enhancement of the absorption in this region. However, at these compressed bond distances, the excited state becomes more delocalized and both the cluster model and the ΔSCF method become unreliable.

In summary, we have unraveled the nature of the optical absorption spectrum of Li_2O_2 using a combination of many-body perturbation theory for extended systems and an embedded cluster model. It has been shown that the Li_2O_2 spectrum at low energies can be understood in terms of a localized exciton at the O_2^{2-} peroxide ion strongly coupled with its breathing vibrational mode. The origin of this localization is the decoupled nature of the O_2^{2-} ions from the rest of the lattice. Indeed Li_2O_2 could be seen as a molecular solid formed by independent O_2^{2-} ions in a "sea" of Li^+ ions. This picture suggests that localization and polaronic effects should be important for the charge transport in Li_2O_2, which could explain the limited performance of Li-air batteries. Further work along these lines is currently ongoing.

J.M.G.L. and K.S.T. acknowledge support from the Lundbeck Foundation's Center for Atomic-scale Materials Design and the Danish Center for Scientific Computing. The authors thank Alan Luntz and Bob Shelby from IBM-Almaden Research for useful discussions and critical reading of the manuscript.

[1] K. M. Abraham and Z. Jiang, J. Electrochem. Soc. **143**(1), 1 (1996).
[2] T. Ogasawara, A. Debart, M. Holzapfel, P. Novak, and P. G. Bruce, J. Am. Chem. Soc. **128**(4), 1390 (2006).
[3] G. Girishkumar, B. McCloskey, A. C. Luntz, S. Swanson, and W. Wilcke, J. Phys. Chem. Lett. **1**(14), 2193 (2010).
[4] B. D. McCloskey, D. S. Bethune, R. M. Shelby, G. Girishkumar, and A. C. Luntz, J. Phys. Chem. Lett. **2**(10), 1161 (2011).
[5] H. H. Eysel and S. Thym, Z. Anorg. Allg. Chem. **411**(2), 97 (1975).
[6] J. Z. Chen, J. S. Hummelshoj, K. S. Thygesen, J. S. G. Myrdal, J. K. Norskov, and T. Vegge, Catal. Today **165**(1), 2 (2011).
[7] T. R. Griffiths, K. A. K. Lott, and M. C. R. Symons, Anal. Chem. **31**(8), 1338 (1959).
[8] T. Andersen and J. L. Baptista, Phys. Status Solidi B **44**(1), 29 (1971).
[9] P. Kubelka and F. Munk, Ann. Tech. Phys. **11**, 593 (1931).
[10] E. E. Salpeter and H. A. Bethe, Phys. Rev. **84**(6), 1232 (1951).
[11] G. Onida, L. Reining, and A. Rubio, Rev. Mod. Phys. **74**(2), 601 (2002).
[12] L. Hedin, Phys. Rev. **139**(3A), A796 (1965).
[13] R. W. Godby and R. J. Needs, Phys. Rev. Lett. **62**(10), 1169 (1989).
[14] L. Chiodo, J. M. Garcia-Lastra, A. Iacomino, S. Ossicini, J. Zhao, H. Petek, and A. Rubio, Phys. Rev. B **82**(4), 045207 (2010).
[15] See http://www.quantum-espresso.org/ for the details of Quantum Espresso Package.
[16] L. G. Cota and P. de la Mora, Acta Crystallogr. **61**, 133 (2005).
[17] J. P. Perdew, K. Burke, and M. Ernzerhof, Phys. Rev. Lett. **77**(18), 3865 (1996).
[18] H. J. Monkhorst and J. D. Pack, Phys. Rev. B **13**(12), 5188 (1976).
[19] A. Marini, C. Hogan, M. Gruning, and D. Varsano, Comput. Phys. Commun. **180**(8), 1392 (2009).
[20] J. S. Hummelshoj, J. Blomqvist, S. Datta, T. Vegge, J. Rossmeisl, K. S. Thygesen, A. C. Luntz, K. W. Jacobsen, and J. K. Norskov, J. Chem. Phys. **132**(7), 071101 (2010).
[21] Y. N. Zhuravlev, N. G. Kravchenko, and O. S. Obolonskaya, Russ. J. Phys. Chem. B **4**(1), 20 (2010).
[22] H. Wu, H. Zhang, X. Cheng, and L. Cai, Philos. Mag. **87**(23), 3373 (2007).
[23] G. T. Velde, F. M. Bickelhaupt, E. J. Baerends, C. F. Guerra, S. J. A. Van Gisbergen, J. G. Snijders, and T. Ziegler, J. Comp. Chem. **22**(9), 931 (2001).
[24] J. M. Garcia-Lastra, J. Y. Buzare, M. T. Barriuso, J. A. Aramburu, and M. Moreno, Phys. Rev. B **75**(15), 155101 (2007).
[25] E. Condon, Phys. Rev. **28**(6), 1182 (1926).